Frequency-dependent seismic reflection coefficient for discriminating gas reservoirs

Duo Xu [1,2] , Yanghua Wang [1], Qigan Gan[2], Jianming Tang [2]

1. Centre for Reservoir Geophysics, Imperial College London, UK
2. E&P Research Institute of Southwest Petroleum Company, Sinopec, China

Abstract

The asymptotic equation of wave propagation in fluid-saturated porous media is available for calculating the normal reflection coefficient within seismic frequency band. This frequency-dependent reflection coefficient is expressed in terms of a dimensionless parameter ε, which is the product of the reservoir fluid mobility (i.e. inverse viscosity), fluid density, and the frequency of the signal. In this paper, we apply this expression to Xinchang gas-field, China, where reservoirs are super tight sands with very low permeability. We demonstrate that the variation in reflection coefficient at gas/water contacts is observable within seismic frequency band. Then we conduct seismic inversion to generate attributes which first indicate the existence of fluid (either gas or water), and then discriminate a gas reservoir from a water reservoir.

Keywords: normal reflection coefficient, poroelastic media, gas/water contact, chaotic inversion

1. Introduction

Hydrocarbon reservoirs as well as many other sedimentary rocks are fluid-saturated porous materials, in which the elastic properties can be described by a poroelasticity theory that predicts the effects of pore fluid movements relative to the solid skeleton on seismic waves propagating through the rock. However, most of poroelastic studies are focused on velocity dispersion and attenuation, few researchers consider plane-wave reflection coefficients in the porous media. In this paper, we design a gas/water contact model based on petrophysical parameters collected from Xinchang gas-field, Southwesten China, and investigate the potential frequency-dependency of the normal-incident reflection coefficient within the seismic frequency band.

The classic theory of poroelasticity (Biot, 1956a, b, Dvorkin , 1993) is not suitable for the seismic which has low frequency less than 100 Hz. Its predicted wave attenuation and dispersion only become significant at frequencies comparable to the so-called Biot's characteristic frequency, which is usually 0.1 MHz or higher (Gurevich, 2004). The relative fluid movement at low frequencies is negligible and the rock behaves like an elastic solid with the equivalent elastic moduli given by Gassmann's (1951) equation.

In practice, fractures may have a significant impact on the flow properties of the reservoirs.

Dual-porosity model, proposed originally by Barenblatt *et al*. (1960), considers the presence of fractures at different scales of permeability. A connected system of fractures, due to relatively simple geometry of the pore space, is highly permeable for fluid flow. The matrix, due to the tortuous pores and pore throats, is significantly less permeable. At the same time, the total volume of fractures is usually small and the matrix blocks contain most part of the reservoir fluid.

However, according to Barenblatt model, the fluid flow in matrix blocks is local: it only supports the exchange of fluid between individual blocks and the surrounding fractures. In large scale, fluid flows through fractures only. Pride and Berryman (2003 a & b) proposed another dual-porosity model which supports large-scale fluid flow in both media. This model combined Barenblatt model with Biot's theory of poroelasticity and has the applicability not limited to fractured rocks (Goloshubin, 2006, 2008). But to cases whenever the permeability of the rock has two or more contrast scales. These scales must be distributed in the medium in such a way that every representative volume comprises both a small-volume highly permeable medium and a low-permeable analog of matrix.

In order to understand and to explore implications for reflections from an interface between two porous media, it is desirable to obtain analytical expressions for the reflection coefficients. However, they are too complicated for arbitrary incidence angles (Denneman *et al*., 2002). The problem is greatly simplified for the normal incidence. Based on Biot-Barenblatt poroelastic model, Silin and Goloshubin (2006, 2010) derived an asymptotic expression for the reflection and transmission coefficients. These asymptotic expressions are approximate but have a relatively simple mathematical form. They are valid in the low-frequency end of the spectrum including the seismic frequency band (10–100 Hz), for a plane wave crossing a permeable interface at a normal incident angle. In this paper, we investigate the potential applicability of this normal-incidence reflection coefficient to the gas/water contact models in a gas-field.

2. Petrophysical model of study area

The study area is Xinchang gasfield, Southwesten China (Gan *et al*., 2008). Table 1 lists petrophysical parameters in this area. We collect these parameters from rock physics measurements and well-log data. When we calculate the reflection coefficient, we assume parameters of skeleton to be same for up and down porous layers.

In Xinchang area, the reservoirs are tight sand with very low permeability. The average permeability of a target reservoir is about 0.03 millidarcy. The production is mainly the nature gas, which is mostly from fractures. When the fractures occur in the reservoir, permeability will increase drastically up to decades or hundreds fold of it. Therefore, in the following numerical calculation, we design two permeability parameters (0.03 and 30 mD) in the model. The permeability of 30 mD corresponds to the case with fractures present.

The petrophysical model includes the following parameters:

K_g : bulk module of grains solid,

K : the bulk module of the porous medium,

μ : the shear module,

ϕ : porosity,

κ : permeability,

ρ_g : the density of grains,

K_f : the fluid module,

ρ_f : the fluid density,

η : the steady-state shear viscosity.

Table 1. Properties of the porous rock and the sample pore fluid.

(1) Parameters of the porous rock

	K_g (GPa)	K (GPa)	μ (GPa)	ϕ	κ (mD)	ρ_g (kg.m^{-3})
Sand	38	24.1	16.6	0.10	0.03 or 30	2650

(2) Parameters of the pore fluid

	K_f (GPa)	ρ_f (kg.m^{-3})	η (Pa.s)
Water	2.22	1000	0.001
Gas	0.0001	140	1.0×10^{-5}

3. Normal-incidence reflection coefficient at a gas-water contact

Consider two half-spaced poroelastic media, labeled by superscripts a and b (Figure 1), separated by a permeable plane interface at $z = 0$. For an incident fast wave arriving from the half-space $z < 0$, there are four waves to be generated: reflected fast and slow waves, and transmitted fast and slow waves.
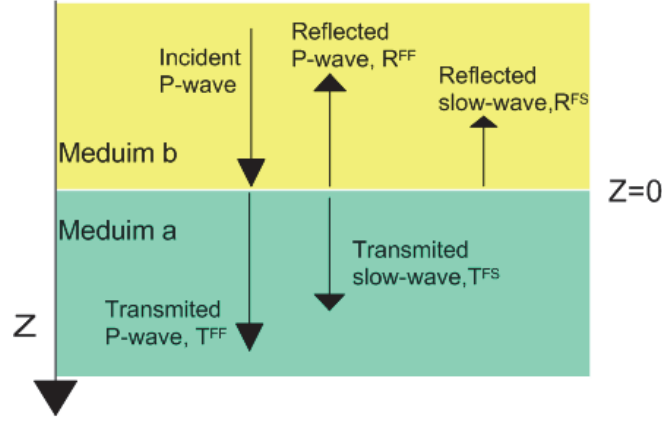

Figure 1. A fast wave incidental from the half-space $z < 0$ generates four waves generates four waves at a planar interface: reflected fast and slow waves and transmitted fast and slow waves.

The mass and momentum balance imply that the skeleton displacement, the Darcy velocity of the fluid, the total stress, and the fluid pressure must be continuous at the interface. The asymptotic expressions of normal-incidence reflection and transmission coefficients from this interface are (Silin and Goloshubin, 2010)

$$R^{FF} = R_0^{FF} + R_1^{FF} \varepsilon , \qquad (1)$$

$$T^{FF} = T_0^{FF} + T_1^{FF} \varepsilon , \qquad (2)$$

where R_0^{FF}, T_0^{FF}, R_1^{FF} and R_1^{FF} are the zero- and first-order terms, and ε is an integrated parameter defined as

$$\varepsilon = e^{i\pi/4} \sqrt{\left|\frac{\rho_f \kappa \omega}{\eta}\right|} . \tag{3}$$

which combines the fluid density ρ_f, the fluid viscosity η, and the permeability κ. Note here that we have redefined parameter ε in slightly different way from Silin and Goloshubin (2010), so that we are able to present the expressions in a linear form.

In the asymptotic expansions, the zero-order terms are given by

$$R_0^{FF} = \frac{Z_b^{FF} - Z_a^{FF}}{Z_b^{FF} + Z_a^{FF}} , \tag{4}$$

$$T_0^{FF} = 1 + \frac{Z_b^{FF} - Z_a^{FF}}{Z_b^{FF} + Z_a^{FF}} . \tag{5}$$

where Z is a modified acoustic impedance

$$Z = \frac{M}{v_p} \sqrt{\frac{\gamma_\beta + \gamma_K^2}{\gamma_\beta}} , \tag{6}$$

expressed in terms of (Biot, 1962)

$$\gamma_\beta = K \left(\frac{1}{K_f} \phi + \frac{K_g - K}{K_g^2}(1-\phi) \right),$$

$$\gamma_K = 1 - \frac{K}{K_g}(1-\phi)^2,$$

$$v_p = \sqrt{\frac{K + \frac{4}{3}\mu}{\phi\rho_f + (1-\phi)\rho_g}} .$$

The coefficients of the first-order terms are defined by

$$R_1^{FF} = \frac{Z_b(T_1^{FS} - R_1^{FS})}{Z_b + Z_a} , \tag{7}$$

$$T_1^{FF} = \frac{Z_a(R_1^{FS} - T_1^{FS})}{Z_b + Z_a} . \tag{8}$$

In these coefficients, the slow-wave reflection and transmission coefficients are

$$R_1^{FS} = \frac{2Z_b Z_a}{D(Z_b + Z_a)}\left(\frac{\gamma_{Kb}(\gamma_{Ka}^2 + \gamma_{\beta a})}{\gamma_{Ka}(\gamma_{Kb}^2 + \gamma_{\beta b})} - 1\right),\tag{9}$$

$$T_1^{FS} = \frac{2Z_b Z_a}{D(Z_b + Z_a)}\left(1 - \frac{\gamma_{Ka}(\gamma_{Kb}^2 + \gamma_{\beta b})}{\gamma_{Kb}(\gamma_{Ka}^2 + \gamma_{\beta a})}\right),\tag{10}$$

where

$$D = \frac{1}{\sqrt{\gamma_\kappa}}\frac{M_a}{v_{fa}}\frac{\gamma_{Kb}^2 + \gamma_{\beta b}}{\gamma_{Kb}}\frac{\sqrt{\gamma_{Ka}^2 + \gamma_{\beta a}}}{\gamma_{Ka}} + \frac{M_b}{v_{fb}}\frac{\gamma_{Ka}^2 + \gamma_{\beta a}}{\gamma_{Ka}}\frac{\sqrt{\gamma_{Kb}^2 + \gamma_{\beta b}}}{\gamma_{Kb}},$$

and $v_f = \sqrt{M/\rho_f}$.

We use equation (1) to calculate the reflection coefficient at a gas/water contact in Xinchang gasfield. As ε is the function of frequency ω, the reflection coefficient is frequency dependent. We calculate the variation of reflection coefficient versus frequency $\omega \neq 0$ by $\Delta R = 100\,|\,(R(\omega) - R_0)/R_0\,|$ (in percentage), where $R_0 \equiv R(\omega = 0)$ is the reflection coefficient for frequency $\omega = 0$.
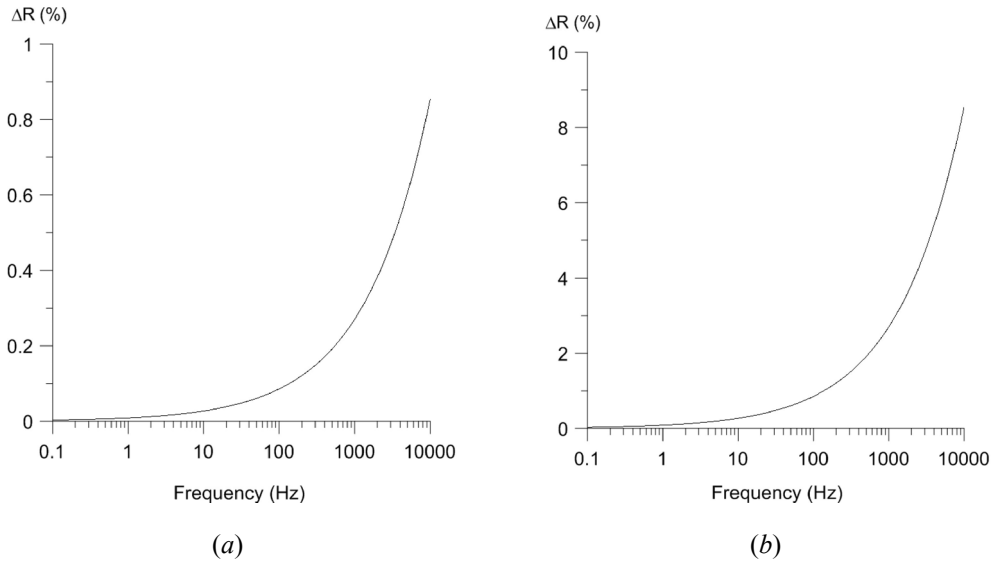

Figure 2. The variation (in percentage) of reflection coefficient at an interface between gas-saturated porous medium and water-saturated medium in Xinchang gasfield. (*a*) The permeability $\kappa = 0.03$ mD. (*b*) The permeability $\kappa = 30$ mD. The calculation is based on formula (1). The incident wave is from gas-saturated porous medium.

When the permeability is very low at 0.03 mD, there is very small change in reflection coefficient at the gas/water interface (Figure 2a). However, when there are fractures presented in porous medium, sometimes the permeability can be very big (2 to 3 magnitude orders higher) within strongly fractured media in Xinchang area. When the permeability increases to 30 mD, there is about 1% of the reflection coefficient change within seismic frequency band (Figure 2b).

The key factor which makes the asymptotic expression of the normal incident reflection

coefficient work in seismic band is the consideration of dynamic and non-equilibrium effects in fluid flow (Silin and Goloshubin, 2010). Modified Darcy's law is

$$W + \tau \frac{\partial W}{\partial t} = -\frac{\kappa}{\eta}\left(\nabla p + \rho_f \frac{\partial^2 u}{\partial t^2} \right) \qquad (11)$$

where W denotes the Darcy velocity of the fluid relative to the skeleton, τ is a parameter having the dimensionality of time, and p is the pressure of fluid. The additional term $\tau\,\partial W / \partial t$ to the Darcy's law expresses dynamic and non-equilibrium effects in fluid flow. This modification of Darcy's law is equivalent to a linearization of the dynamic permeability for a periodic oscillatory flow (Johnson *et al*., 1987; Cortis, 2002; Carcione, 2003). But derived asymptotic expressions have a simple mathematical form which is useful in practice.

Under the asymptotic model, increasing the frequency would enlarge the variation of reflection response at the interface between two porous mediums. So problems of reflection coefficient at gas/water contact with low permeability such as Xinchang gasfield will partially subject to the development of high-resolution seismic exploration, and to the enhancement of any existed seismic data sets, by high-fidelity seismic inverse Q filtering (Gan *et al*., 2008).

4. Seismic inversion for fluid discrimination

The positive change in reflection coefficient in (Figure 2) provides us an opportunity to invert for the reflectivity based on formula (1). Here, we rewrite formula (1) as

$$R^{FF}(\omega) = R_0^{FF} + C_1(1+i)\sqrt{\omega} \quad , \qquad (12)$$

where the constant

$$C_1 = R_1^{FF}\sqrt{\left|\frac{\rho_f \kappa}{2\eta}\right|} \, .$$

It reflects proportionally the mobility (inverse viscosity) of reservoir fluid, the density of fluid, and the permeability.

We use a chaotic optimization algorithm to invert for parameters R_0^{FF} and C_1. The inversion object function is defined as

$$J = \sum_\omega [R^{FF}(R_0^{FF}, C_1, \omega) - R_{\mathrm{obs}}(\omega)]^2 \quad , \qquad (13)$$

where R_{obs} is the observed field data in the frequency domain. Chaos as a universal phenomenon is stochastic but ergodic and regular (Lorenz, 1993). One can exploit the ergodicity as a mechanism for global optimization, to effectively avoid the search being trapped in local optimum.

This is a nonlinear algorithm searching for an optimal random variable x which is made by Logistic mapping equation

$$x^{(k+1)} = \mu x^{(k)}(1 - x^{(k)}), \qquad (14)$$

where k is the iteration number, and μ is a constant that controls stochastic behavior. If $3.569 \le \mu \le 4$, the random variable x is chaotic. In our inversion here, we set $\mu = 4$. The

dimensionless x value is in the range (0, 1). However, the following three points (0.25, 0.5, 0.75), for which the variable x is unchangeable should be excluded from the iteration. If we have n of unknown parameters $\{x_i, i = 1, 2, \cdots, n\}$ that need to be inverted, we simply set different initial value for each parameter x_i.
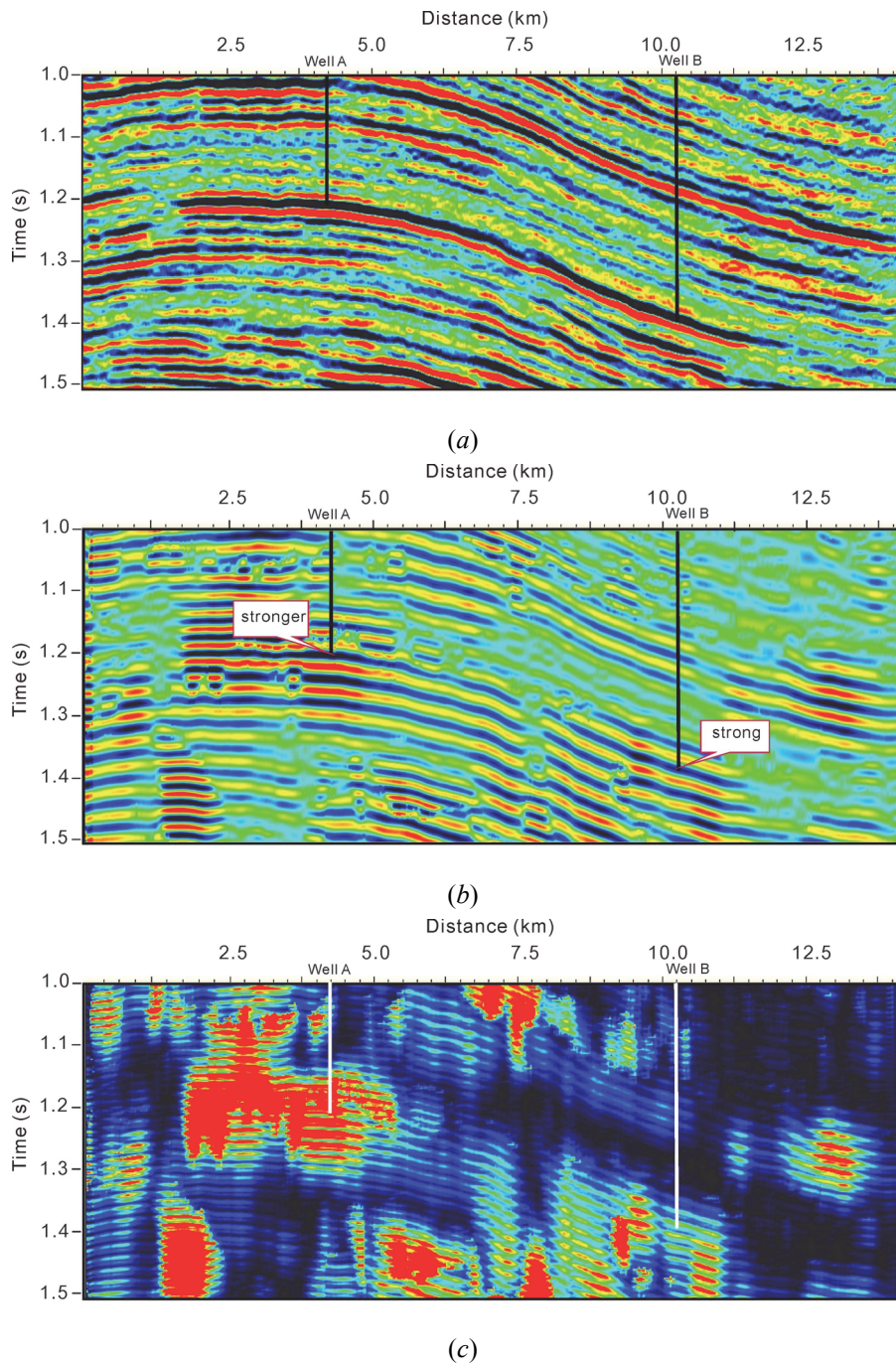

(a)

(b)

(c)

Figure 3. (a) A seismic section in Xingchang gasfield. This section crosses two wells, where the end of well A is a gas reservoir and the end of well B is a water reservoir.   (b) Inverted C_1 attribute section by chaotic optimization. (c) The attribute variation calculated by $C_1^2 \Delta |C_1|$. Strong amplitude means more mobility. Gas reservoir shows stronger amplitude than water reservoir in the same formation.

For each iteration k, given any random variable $x_i^{(k)}$ in the range (0, 1), we scale-up to actual magnitude in its physical space through

$$\hat{x}_i^{(k)} = a_i + (b_i - a_i)x_i^{(k)}, \tag{15}$$

where $\hat{x}_i^{(k)}$ is the actual model parameter in the model space. The range of $\hat{x}_i$ is in $[a_i, b_i]$, with a physical units "*model*". We substitute all n parameters $\{\hat{x}_i^{(k)}, i = 1,2,\cdots,n\}$ simultaneously to the objective function within each iteration. Eventually, we can find the solution which minimizes the objective function.

Figure 3a is the field seismic section from Xinchang gas-field, the reservoir (the trough in Figure 3a) is relative shallow with low impendence. This section cross two wells: the end of well A is a gas reservoir, and the end of well B is a water reservoir.

Figure 3b is the inverted C_1 section. This attribute section has different features from Figure 3a. In seismic section (Figure 3a), we couldn't find the difference at the location of well A and well B in the reservoir. However, in Figure 3b, we can observe the differences: (a) The amplitude is stronger at well A than it at the well B. (2) Meanwhile, both of them have stronger amplitude than other areas. The big value of C_1 means strong mobility of fluid, when there is gas or water present in the reservoir, the amplitude of C_1 will become strong. In addition, relatively stronger amplitude indicates the existence of gas at well A.

In order to highlight the variation in the attribute C_1, we calculate a weighted attribute $C_1^2 \Delta |C_1|$, where $\Delta |C_1|$ is the difference of the absolute value $|C_1|$ between two adjunct samples. As shown in Figure 3c, the response of the gas reservoir is clearer than the response of the water reservoir.

In summary, the strong amplitude in C_1 indicates the mobility of fluid (either gas or water), and the strong amplitude in $C_1^2 \Delta |C_1|$ indicates the existence of gas reservoir.

5. Conclusions

The asymptotic equation of seismic reflection is available for calculating the normal reflection coefficient within seismic frequency band at a gas/water contact. The reflection coefficient is expressed as a power series with respect to a small dimensionless parameter ε, which is the product of the reservoir fluid mobility and density, and the frequency of the signal. The functional structure of these coefficients provides opportunities for frequency-dependent seismic inversion, to produce frequency-dependent seismic attributes.

We have demonstrated that in Xinchang gas field where reservoirs are super tight sands with very low permeability, the variation in reflection coefficient at gas/water contacts can still be observed within seismic band. Further more, seismic inversion generated attributes C_1 indicates the existence of fluid, and weighted absolute value $C_1^2 \Delta |C_1|$ discriminates a gas reservoir from water reservoir.

References

Biot M. A., 1956a. Theory of propagation of elastic waves in a fluid-saturated porous solid, I:

low-frequency range. *J. Acoust. Soc. Am*. **28**, 168–78.

Biot M. A., 1956b. Theory of propagation of elastic waves in a fluid-saturated porous solid, II: higher frequency range. *J. Acoust. Soc. Am*. **28**, 179–91.

Biot, M. A., 1962. Mechanics of deformation and acoustic propagation in porous media. *Journal of Applied Physics*, **33**, 1482–98.

Denneman A. I. M., Drijkoningen G. G., Smeulders D. M. J. and Wapenaar K., 2002. Reflection and transmission of waves at a fluid/porous-medium interface. *Geophysics* **67**, 282–91.

Dvorkin J. and Nur A., 1993. Dynamic poroelasticity: A unified model with the squirt and the Biot mechanisms. *Geophysics* **58**, 524–33.

Gan Q., Xu D., Tang J. and Wang Y., 2009. Seismic resolution enhancement for tight-sand gas reservoir characterization. *Journal of Geophysics and Engineering* **6**, 21–8.

Gassmann F., 1951. Über die Elastizität poröser Medien. *Vierteljahrscr. Nat. Ges. Zür*. **96**, 1–23.

Goloshubin G. M. and Silin D. B., 2006. Using frequency-dependent seismic attributes in imaging of a fractured reservoir. *Expanded Abstracts*, 76th SEG Annual Meeting, New Orleans, 1742–6.

Goloshubin G. M., Korneev V. A., Silin D. B., Vingalov V. M. and van Schuyver C., 2006. Reservoir imaging using low frequencies of seismic reflections. *The Leading Edge* **25**, 527–31.

Goloshubin G., Silin D., Vingalov V., Takkand G. and Latfullin M., 2008. Reservoir permeability from seismic attribute analysis. *The Leading Edge* **27**, 376–81.

Gurevich B., Ciz R., Denneman A. I. M., 2004. Simple expressions for normal incidence reflection coefficients from an interface between fluid-saturated porous materials. *Geophysics* **69,** 1372–7.

Lorenz E., 1993. *The Essence of Chaos*. (Seattle: University of Washington Press).

Pride S. R. and Berryman J. G., 2003a. Linear dynamics of double-porosity dual-permeability materials, I: Governing equations and acoustic attenuation. *Phys. Rev. E* **68**, 1–10.

Pride S. R. and Berryman J. G., 2003b. Linear dynamics of double-porosity dual-permeability materials, II: Fluid transport equations. *Phys. Rev. E* **68**, 1–10.

Silin D. B., Korneev V. A., Goloshubin G. M. and Patzek T. W., 2006. Low-frequency asymptotic analysis of seismic reflection from a fluid-saturated medium. *Transp. Porous Media* **62**, 283–305.

Silin D. B. and Goloshubin G. M., 2010. An asymptotic model of seismic reflection from a permeable layer. *Transp. Porous Media* **83**, 233–56.